Graphical Abstract

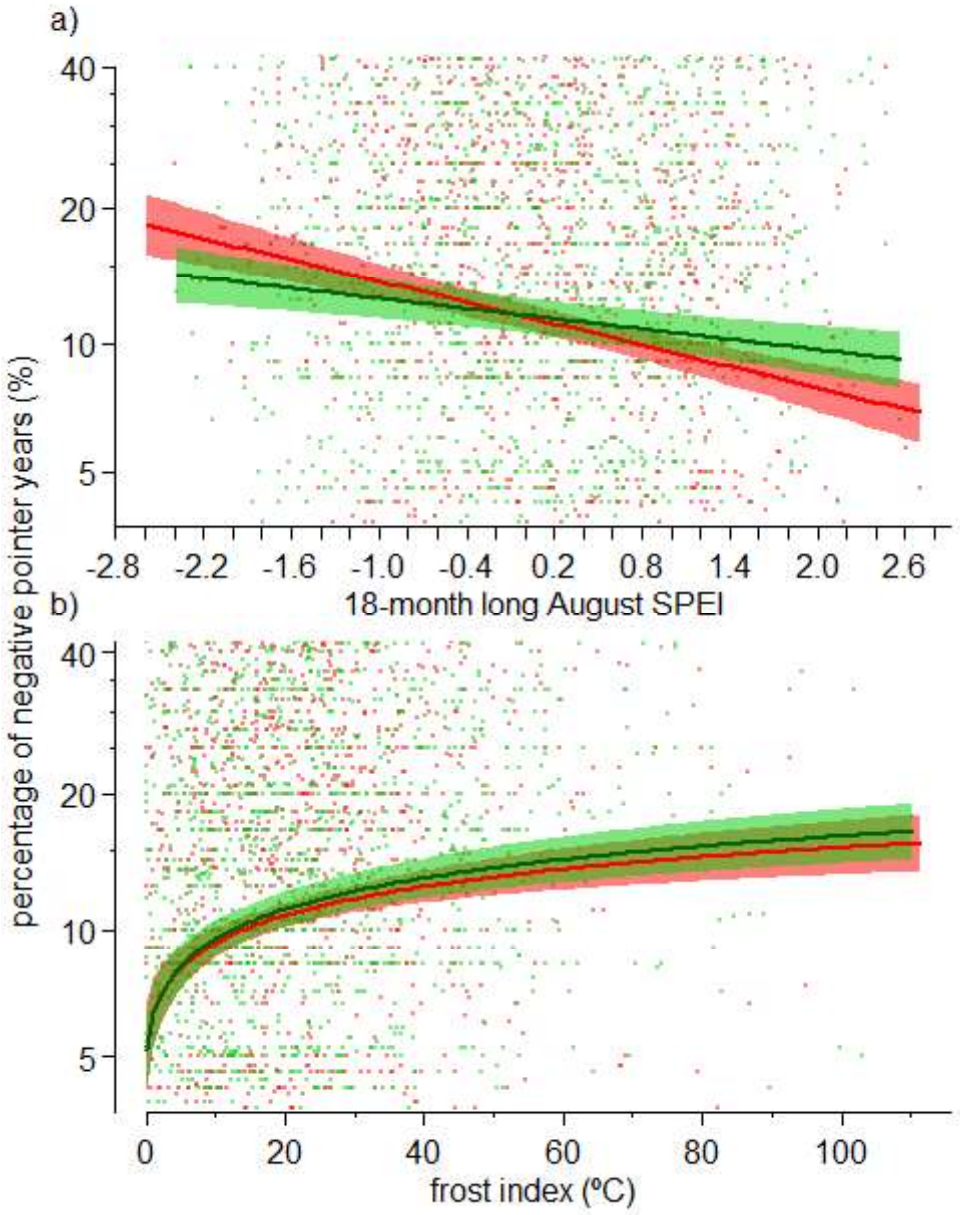

Graphical abstract. Effects of drought (18-month long August SPEI) and frost index on the percentage of negative pointer years in Silver fir (red lines and symbols) and European beech (green lines and symbols) across their southern distribution limit in north-eastern Spain.

Highlights

- Droughts and frosts impact growth in species southernmost distribution limits.
- Droughts and frosts impair Silver fir and European beech radial growth.
- Silver fir growth is more affected by drought than by late frosts.
- European beech growth is more affected by late frosts than by drought.
- We could not find interactive effects of drought and late frosts on growth.

Summer drought and spring frost, but not their interaction, constrain European beech and Silver fir growth in their southern distribution limits

Antonio Gazol[1,2,3], J. Julio Camarero[3], Michele Colangelo[3,4], M. de Luis[5], E. Martínez del Castillo[5] and Xavier Serra-Maluquer[3]

[1]Departamento de Biología y Geología, Física y Química Inorgánica, Universidad Rey Juan Carlos, C/ Tulipán s/n, 28933, Móstoles, Spain.
[2]Basque Centre for Climate Change (BC3), Sede Building 1, 48940 Leioa (Spain).
[3]Instituto Pirenaico de Ecología (IPE-CSIC), Avda. Montañana 1005, 50192 Zaragoza, Spain
[4]School of Agricultural, Forest, Food and Environmental Sciences, Univ. Basilicata, Potenza, Italy
[5]Department of Geography and Spatial Management, University of Zaragoza, Zaragoza, Spain

*Corresponding author:
J. Julio Camarero
Instituto Pirenaico de Ecología (IPE-CSIC)
Avda. Montañana 1005
50059 Zaragoza, Spain
E-mail: jjcamarero@ipe.csic.es

Summary

Climate warming has lengthened the growing season by advancing leaf unfolding in many temperate tree species. However, an earlier leaf unfolding increases also the risk of frost damage in spring which may reduce tree radial growth. In equatorward populations of temperate tree species, both late frosts and summer droughts impose two constraints to tree growth, but their effects on growth are understudied. We used a tree-ring network of 71 forests to evaluate the potential influence of late frosts and summer droughts on growth in two tree species that reach their southern distribution limits in north-eastern Spain: the deciduous European beech (*Fagus sylvatica* L.) and the evergreen Silver fir (*Abies alba* Mill). The occurrence of late frost events and summer drought was quantified by using a high-resolution daily temperature and precipitation dataset considering the period 1950-2012. Late frosts were defined as days with average temperature below 0ºC in the site-specific frost-free period, whereas drought was quantified using the 18 month-long August Standardized Precipitation Evapotranspiration Index (SPEI). The growth of European beech and Silver fir was reduced by the occurrence of both late frost events and summer drought. However, we did not find a significant interaction on growth of these two climate extremes. Beech was more negatively impacted by late frosts, whereas Silver fir was more impacted by summer drought. Further studies could use remote-sensing information or in situ phenological records to refine our frost index and better elucidate how late frosts affect growth, whether they interact with drought to constrain growth, and how resilience mechanisms related to post-frost refoliation operate in beech.

Key words: *Abies alba*; dendroecology; *Fagus sylvatica*; late frosts; phenology; Pyrenees.

Introduction

In temperate and Mediterranean biomes, climate has warmed during the last decades (IPCC, 2013) increasing the length of the growing season and advancing leaf unfolding in many tree species (Menzel et al., 2006; Keenan et al., 2014; Fu et al., 2015). While a longer growing season may lead to an earlier leaf unfolding and potentially enhance tree radial growth (Čufar et al., 2015), it might also be a double-edged sword. Advanced leaf-flushing may allow lengthening the growing season through an earlier onset in spring, when water is not limiting (Sánchez-Gómez et al., 2013). Nevertheless, an advanced leaf unfolding increases the risk of frost damage as has been observed in boreal, continental, temperate and mountain forests (Hänninen, 1991; Augspurger, 2009, 2013; Utkina and Rubtsov, 2017; Vitasse et al., 2018). Current climate projections suggest the increase in the frequency of extreme climate events such late frosts but also droughts and heat weaves (IPCC, 2013), which may negatively impact forest productivity and functioning (Frank et al., 2015).

In the worst scenario, the simultaneous occurrence of spring late frosts together with summer droughts in the same growing season might limit forest productivity by reducing tree radial growth (Rubtsov et al., 2008; Vanoni et al., 2016). This could be the case of several major European tree species dominants in temperate regions such as Silver fir (*Abies alba* Mill., hereafter silver fir) and European beech (*Fagus sylvatica* L., hereafter beech), which reach their southernmost distribution limit in north-eastern Spain mountains where growth is impaired by low temperatures but also by summer drought (Rozas, 2003; Camarero et al. 2015a, 2015b; Gazol et al,. 2015; Martinez del Castillo et al., 2016; Gazol et al., 2018; Martinez del Castillo et al., 2019ab). In such transitional regions between temperate and drought-prone Mediterranean conditions, a trade-off may exist between late frost tolerance and summer-drought resistance (Robson

et al., 2013). Thus, understanding how temperate tree species as Silver fir and beech respond to the potentially synergic effects of late frosts and summer droughts in their southernmost distribution limit may help to understand the future performance of these species in sight of the climate-change increased air temperature variability.

Late frost damage depends on budburst and leaf-flushing dates and increases with the occurrence of frost events in early spring combined with previous mild temperatures which enhance leaf unfolding (Hänninen, 1991). Frost can damage recently expanded leaves when occurring after leaf-flushing (Augspurger, 2009, 2013; Vitasse et al., 2014a, 2014b), limiting photosynthesis and carbon uptake in spring and subsequently radial growth (Dittmar et al., 2006; Vanoni et al,. 2016; Príncipe et al., 2017). Quantifying the effect of late frost damage on radial growth is complicated since phenological records are required to identify how a frost event damages plant tissues. In the absence of such data, the occurrence of frost events in late spring can serve as a proxy to identify the potential impact of late frost events on tree growth (e.g. Vanoni et al., 2016). In this sense, it has been argued that the negative impacts of late frost occurrence on growth may increase polewards (Weigel et al., 2018) and upwards (Vitasse et al., 2018), which suggests that forests located at higher elevation will be the most negatively impacted. However, these assumptions are not supported by recent research. First, European maritime and coastal areas seem to be more exposed to more severe late spring frosts than continental areas (Ma et al., 2019). In addition, climate warming may blur thermal gradients and lead to a more uniform phenology regardless elevation (Chen et al., 2018). Finally, tree species may present enough growth plasticity, or even local genetic adaptations, to override the negative consequences of late frost events on growth (Puchałka et al., 2017).

Whether tree controls on leaf-flushing date is evolutionary linked to the occurrence of late frost events also remains an open debate (Hofmann and Bruelheide, 2015; Körner et al., 2016; Lenz et al., 2016; Vitra et al., 2017), but what is clear is that not all tree species are at the same risk of late frost damage as flushing dates and frost resistance capacity vary across species and populations (Lenz et al., 2016; Bigler and Bugmann, 2018). For example, studies performed in Eastern Europe have identified the existence of different phenological forms in pedunculate oak (*Quercus robur* L.) according to their leaf-flushing behaviours (Rubtstov and Utkina, 2008; Utkina and Rubtsov, 2017). Early-flushing oaks avoid summer drought at a cost of higher frost risk in spring, whilst late-flushing oaks avoid spring frosts but have a shorter growing period. The growth balance of the two phenological forms is similar (Rubtstov & Utkina, 2008). Leaf-out timing of beech occurs earlier than in other co-occurring species, probably because leaf-out is partially controlled by photoperiod in this species, reducing its responsiveness to late-spring frosts (Lenz et al. 2013, 2016; Ma et al., 2018). However, the existence of different phenological forms in relation to leaf flushing dates has been also suggested in the case of beech (Kraj and Sztorc, 2009). In the case of Silver fir, young individuals growing in the shade showed a delayed dormancy break compared to trees growing in the sun which resulted in a reduced impact of late frost damage on leaves and shoots (Spulak and Martincova, 2015). In both tree species, late frost events result in radial growth reductions (Dittmar et al., 2006; Latreille et al., 2017; Príncipe et al., 2017) despite it is expected that the growth of the deciduous beech should be more negatively impacted by spring frost than that of the evergreen Silver fir (Cailleret and Hendrik, 2011; Suvanto et al., 2017). However, warm conditions followed by very low temperatures may also cause needle damage and

123 canopy dieback as trees are exposed to repeated freeze-thaw cycles leading to winter
124 frost drought in conifers (Camarero et al., 2015a).

125 The occurrence of summer drought is one of the main factors impairing tree
126 radial growth, reducing productivity and triggering dieback and high mortality rates
127 worldwide (Anderegg et al., 2012). However, tree responses to drought vary according
128 to species specific physiological characteristics and local adaptations (e.g. Gazol et al.,
129 2018). Both, Silver fir and beech are sensitive to summer drought (Camarero et al.,
130 2018), and they have been found to reduce their radial growth because of summer water
131 shortage in their southernmost populations (Gazol et al., 2015; Rozas et al., 2015;
132 Martinez del Castillo et al., 2019a). In north-east Spain, warming accelerated after the
133 1980s leading to the occurrence of severe droughts (e.g, 1986, 1994-1995, 2005, 2012)
134 causing dieback episodes in both species (Camarero et al., 2015b, 2018; Gazol et al.,
135 2018; Serra-Maluquer et al., 2019). However, the information regarding the occurrence
136 of late frost events in Spain is scarce despite they have been suggested to impact radial
137 growth in Silver fir (Camarero & Gutiérrez 2017).

138 Ongoing climate warming may have resulted in a longer growing season due to
139 earlier budburst and leaf unfolding as has been observed in other European regions (e.g.
140 Vitasse et al., 2018). Phenological records also indicate a generalized advancement of
141 leaf unfolding dates across the Iberian Peninsula (Gordo and Sanz, 2010). Advanced
142 leaf unfolding may enhance growth during early spring and avoid the negative
143 consequences of summer drought at the cost of increasing the exposure to late frost
144 damage (Rubtsov and Utkina, 2008; Kraj and Sztorc, 2009; Puchałka et al., 2017).
145 However, there is also a potential risk that late frost and summer drought may occur in
146 the same growing season, thus synergistically reducing radial growth (Vanoni et al.,
147 2016). How these two climatic factors interact and influence tree growth in the southern

distribution limits of Silver fir and beech remains an open question. In this study, we aim to advance in our understanding of how these two species respond to late frost, summer drought and their interactions. To this end, we used dendrochronological methods to reconstruct the growth of 33 Silver fir and 38 beech stands during the last 60 years across north-east Spain. Daily climate data at a high spatial resolution were used to calculate late frost and to estimate summer drought. We calculated a frost-index based on daily climatic data as we lacked *in situ* information on the phenology of the two species. We expect that: (i) the radial growth of Silver fir and beech is negatively impacted by the occurrence of both, late frost events and summer drought; (ii) beech shows a higher sensitivity to late frosts as compared to silver fir; and (iii) finally, a significant interaction between late frost events and summer droughts impacting growth and indicating that the simultaneous occurrence of these two climate extremes have a stronger impact than their separate incidence.

Material and Methods

Study site and tree species

We studied the radial growth of Silver fir and beech trees in a network of 71 forests (33 silver fir; 38 beech) located in north east Spain (**Figure 1; Table S1 in Supporting Information**). Sampled forests were located in mountain areas (Pyrenees, Pre-Pyrenees and the Iberian Range). The mean annual temperature across the study sites was 8.1 ºC, ranging from 3.4 ºC in the coldest site (Silver fir forest in Panticosa, 1280 m a.s.l.) to 12.4 ºC in the warmest site (beech forest in Bertiz, 405 m a.s.l.). Annual precipitation ranged from 598 mm in the driest site (beech forest in Montsec, 1360 m a.s.l.) to 2738 mm in the wettest site (Silver fir forest in Selva de Oza, 1272 m a.s.l.). All studied sites

172 are located within the biogeographic distribution range of the two species (San Miguel-
173 Ayanz et al., 2016).

174 We chose to study these two species because; (i) their radial growth is sensitive
175 to summer drought and late frost (Dittmar et al., 2006; Gazol et al., 2015, 2018; Rozas
176 et al., 2015); (ii) they often coexist; and (iii) they form their southernmost distribution
177 limits in the studied region. Beech is a deciduous tree widely distributed across
178 European temperate forests, whereas Silver fir is a conifer found in forests with similar
179 climate and soil conditions but mainly restricted to mountain areas and cool-wet sites in
180 the study region (Caudullo et al., 2017).

181

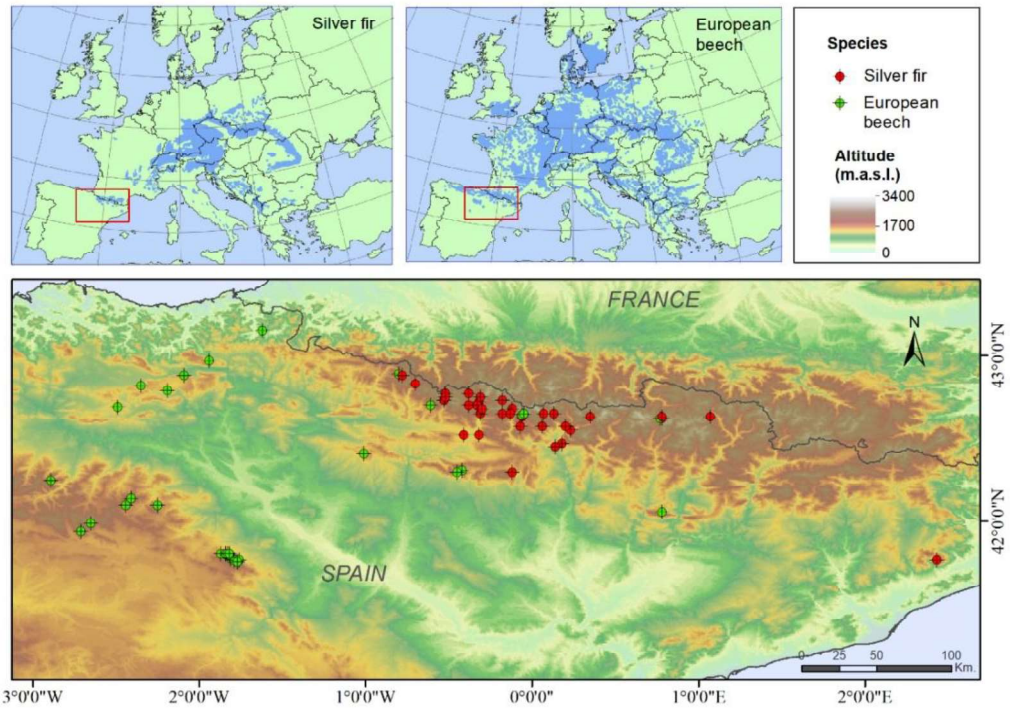

182

183 **Figure 1.** Silver fir (red dots) and European beech (green dots) forests studied in north
184 eastern Spain. The sampled forests are shown together with altitude. The small maps
185 show the distribution of Silver fir and beech in Europe
186 (http://www.euforgen.org/species/) and the location of the study region in north-eastern
187 Spain.

188

189 *Tree-ring width data*

190 In each site, a total number ranging from 10 to 40 dominant or co-dominant trees
191 separated by at least 10 m were randomly selected. Trees were cored at 1.3 m height
192 using Pressler increment borers and two cores were extracted per tree. These cores were
193 air dried in the laboratory and mounted on wooden supports for further processing. The
194 samples were sanded with progressively finer sandpapers until tree rings were clearly
195 visible. Ring widths were measured at 0.01 mm resolution using a LINTAB
196 measurement device (Rinntech, Heidelberg, Germany). Visual cross-dating was
197 performed and checked with the program COFECHA (Holmes, 1983).

198 To quantify the short-term tree growth reductions as a consequence of either late
199 frost events or summer droughts, we calculated the number of individual pointer years
200 at the tree level for the common period for all sites (1950-2012). These individual
201 negative pointer years are annual rings with a substantially smaller width than the *n*
202 preceding annual rings and reflect growth variability at inter-annual scales that may be
203 associated to extreme climate events, such as frosts and droughts (cf. Schweingruber et
204 al., 1990). Individual pointer years were calculated using normalized growth deviations
205 in a 3-year long window, with a >0.75 threshold on the so-called Cropper values
206 (Cropper, 1979). When the negative individual pointer years were identified at the tree
207 level, we quantified the percentage of trees displaying negative pointer years for each
208 particular year in each forest. This result in a temporal series of proportion of trees with
209 negative pointer years in each forest (Table S2 Supporting information).

210

211 *Climate data*

212 We used two recently developed high resolution gridded datasets (5x5 km) of daily
213 precipitation (SPREAD) and maximum and minimum temperatures (STEAD) created

for Spain (Serrano-Notivoli et al., 2017a,b, 2019). For each forest, daily time series (1950-2012) for the closest grid point was selected.

To estimate drought severity at each forest, we calculated the Standardized Precipitation and Evapotranspiration Index (hereafter, SPEI) for the period 1950-2012 (Vicente-Serrano et al., 2010). The SPEI is a measure of drought severity based on temperature and precipitation data and allows comparing drought severity among regions subjected to different climate conditions (Vicente-Serrano et al., 2013). For this reason, we selected SPEI as a measure of drought intensity instead of other metrics such as climatic water balance which are less useful to establish a spatial comparison of drought conditions given the strong climate differences among regions. Negative and positive SPEI values indicate dry and moist conditions, respectively. We calculated 12, 18 and 24-month long summer (June to August) SPEI values for each year, and selected August values because they reflect the maximum cumulative water deficit from the previous to the current growing seasons. In addition, the 18-month long August SPEI was selected because it has a stronger correlation to tree growth than the 12- and 24-month long August SPEIs.

To represent spring late frost events, we created a frost index comparing the averaged minimum daily temperature for the entire study period (1950-2012) with the daily minimum temperature of each particular year (**Supporting Information, Figure S1**). Ideally, the potential influence of spring frost events on tree growth should be quantified accounting for the phenology of the species. That is, dating the leaf unfolding along the study period to quantify the potential occurrence of frost events affecting recently formed plant tissues and spring growth. However, when this information is not available, using climate data as a surrogate can be a valid approach (Vanoni et al., 2016; Vitasse and Rebetez, 2018). The frost index used here quantifies the magnitude of a

239 frost event occurring in a frost-free period (Vanoni et al., 2016). First, we averaged
240 minimum daily temperatures for the entire study period (1950-2012) considering grid
241 overlapping each study site. In this way we obtained the average minimum temperatures
242 from January to December. Second, we quantified the frost-free period by selecting the
243 dates without average minimum temperatures below zero. To avoid potential bias, i.e.
244 dates with average minimum temperatures above zero followed by temperatures below
245 zero, we selected the last date with average minimum temperatures below zero as the
246 starting date of the frost-free period (following Vanoni et al., 2016). In addition, in
247 those sites where the beginning of the frost-free period started before the beginning of
248 March, we forced it to start by early March assuming that growth stopped during winter
249 in both species. This agrees with observation from nearby areas since leaf unfolding in
250 Silver fir starts in mid-April in France (Cuny et al., 2012), and beech leaf unfolding
251 occurs between mid-April and early May in Spain (Gordo and Sanz, 2010). Similarly,
252 we forced the frost-free period to end by late August as done by other authors (Vanoni
253 et al. 2016) because 95% of the growth of the species occurs before August (Ellenberg
254 and Leuschner, 2010; Martinez del Castillo et al., 2016). Finally, we used the daily
255 minimum temperature of each year in the frost-free period to quantify the frost index by
256 summing all values below zero for each particular year. Thus, only those days with
257 temperatures below zero in a period which is historically (1950-2012) frost-free can be
258 considered a late or spring frost event according to our method. This was done in each
259 site to account for the potential differences in frost-free period and frost index across
260 sites.
261
262 *Statistical analyses*

We applied linear mixed-effects models (Pinheiro and Bates, 2000) to study the temporal and spatial variation in the frost index and drought (18 month-long August SPEI). A separate model was created for each variable using the following predictors: calendar year (temporal trend); latitude, longitude and elevation (geographical pattern), averaged mean temperature, and total precipitation (period 1950-2012) and start date of the frost-free period in Julian days (climatic pattern). We included the study site as a random factor (i.e., repeated measures in different years) and the frost index was log-transformed (log (x+1)) prior to analyses in order to achieve normality assumptions. A first-order autocorrelation structure (AR(1)) was included to account for the potential dependence of the frost index and SPEI in year *t* of that in year *t-1* (Zuur et al., 2009).

To identify the set of predictors that better explained the spatiotemporal patterns in frost index and 18 month-long August SPEI we used a multi-model inference approach based on information theory (Burnham and Anderson, 2002). This approach relies on the use of information theory to calculate the relative probability that a given model is more parsimonious than other competing models to explain the response variable. We ranked all potential models according to the second-order Akaike information criterion (AICc). The model showing the lowest AICc value and the largest Akaike weight (w_i, relative probability quantifying if the selected model is the best one) was selected as the best model.

We used different analyses to study the relationship between forest growth and the occurrence of drought and late frost events. First, the Spearman r_s statistic was used to estimate a rank-based measure of association between the, the annual percentage of trees displaying negative pointer years in each site with the 18 month-long August SPEI and the frost index. For each tree species, we studied which factors influenced the correlation between growth (the annual percentage of trees displaying negative pointer

288 years) and drought (18 month-long August SPEI) and between growth and late frosts
289 (frost index). Thus, the above-mentioned correlation coefficients were used as response
290 variables in Generalized Least Squares models (Pinheiro and Bates, 2000). We
291 considered the latitude, longitude, and elevation as well as the maximum, minimum and
292 mean temperature and cumulative precipitation as factors representing the
293 biogeographical gradients of the study region. We also evaluated the second-order
294 polynomial effect of the covariates in order to account for non-linear biogeographic
295 patterns. We ranked all potential models according to the AICc. The model showing the
296 lowest AICc value and the largest w_i was selected as the best model. To quantify the
297 strength of the model, we calculated a pseudo-R^2 (Nagelkerle, 1991).
298 Finally, to generalize the influence of drought and late frost events on growth for
299 each species, we applied Linear Mixed-Effects models (LME; Pinheiro and Bates,
300 2000). Separate models were constructed for each species, using the yearly percentage
301 of negative pointer years in each forest as response variables and the frost index, the 18
302 month-long August SPEI and their interaction as explanatory variables. We included the
303 study site as a random factor since repeated measures (i.e., growth in different years)
304 were obtained for each forest. The percentage of negative pointer years and the frost
305 index were log-transformed (log (x+1)) prior to analyses in order to achieve normality
306 assumptions. A first-order autocorrelation structure (AR(1)) was included to account for
307 the potential dependence of the percentage of negative pointer years in year *t* of that in
308 year *t-1* (Zuur et al., 2009). A graphical examination of the model showed a
309 heterogeneous distribution of residuals (Zuur et al., 2010), and thus a constant variance
310 function structure was included to account for the variation in the occurrence of
311 negative pointer years across sites (Zuur et al., 2009). To identify the set of predictors
312 that better explained the occurrence of negative pointer years in the LMEs (i.e. frost-

index, 18 month-long August SPEI and their interaction) we used a multi-model inference approach based on information theory (Burnham and Anderson, 2002). The model showing the lowest AICc value and the largest w_i was selected as the most parsimonious model. To quantify the strength of the LMEs, we calculated marginal (R^2 which accounts for fixed factors) and conditional (R^2 which accounts for fixed plus random factors) R^2 values (Nakagawa and Schielzeth, 2013).

All statistical analyses were performed in the R statistical environment (R Development Core Team, 2017). The dplR package was used to manage tree-ring width series, detrend them and calculate the chronologies (Bunn et al., 2016). To detect individual pointer years we used the function `pointer.norm` of the package pointRes (van der Maaten-Theunissen et al., 2015). The `lme` function of the 'nlme' package was used to fit the Linear Mixed-Effects models (Pinheiro et al., 2014). The 'MuMIn' package was used to perform the multi-model selection and calculate pseudo-R^2 (Barton, 2012).

Results

The percentage of trees displaying negative pointer years varied between species. Silver fir presented a large percentage of trees (>50%) showing a negative pointer year in 1965, 1984 and 1986 (**Figure 2**). In the case of beech negative pointer years were abundant in 1968, 1994-1995, 1999, 2003, and 2010. Dry conditions (negative 18 month-long August SPEI values) prevailed across sites in years 1986, 1994-1995, and 2005, whereas frost incidence (high values of the frost index) was common in 1975, 1984 and 1991. A marked trend in SPEI towards more negative values (dryer conditions) was observed, whilst frost incidence peaked in the 70´s and decreased after

that. (**Figure 3**). Along this, the results of the LME showed that both, SPEI and frost index has decreased significantly over the last decades (**Table 1**).

The frost index increased with elevation, and decreased with latitude, mean annual temperature and the start of the frost free period (Table 1). The start of the frost-free period (**Figure 4**) was positively related with site longitude ($r = 0.33$; $p < 0.01$), elevation ($r = 0.47$, $p < 0.01$) and annual precipitation ($r = 0.58$, $p < 0.01$), and it was negatively related with the increase in annual temperature ($r = -0.94$, $p < 0.01$). When separated for tree species, the start of the frost-free period was strongly linked to elevation in beech ($r = 0.83$, $p < 0.01$), whereas in the case of Silver fir it was related to latitude ($r = 0.49$, $p < 0.01$). Across sites, beech forests from warm-dry sites from the Iberian Range (e.g. M14FS, 1440 m; **Figure 4**; see also Table S1) showed the highest proportion of negative pointer years (25.7%), whereas in the case of Silver fir this was observed in a central Pyrenean site (FAAA, 918 m).

Table 1. Results of the linear mixed-effects models selected to study the spatiotemporal patterns in drought intensity (18 month-long August SPEI) and frost index. For each variable, the covariates included in the model are displayed (t-statistic). These covariates are: elevation (m a.s.l.), latitude (decimal degrees), mean annual temperature (T Med; in ºC) and beginning of the frost-free period (ffp). The Akaike weight of the model (w_i) and the marginal R^2 values (conditional R^2 values are indicated between parenthesis) are displayed. Significant values are indicated with asterisks (* $p < 0.05$ and ** $p < 0.01$)

	Year	Elevation	Latitude	T Med	ffp	w_i	R^2
SPEI	-15.49**	–	–	–	–	27%	0.15 (0.15)
Frost index	-16.78**	3.10**	-5.47**	-9.05**	-9.71**	22%	0.17 (0.21)

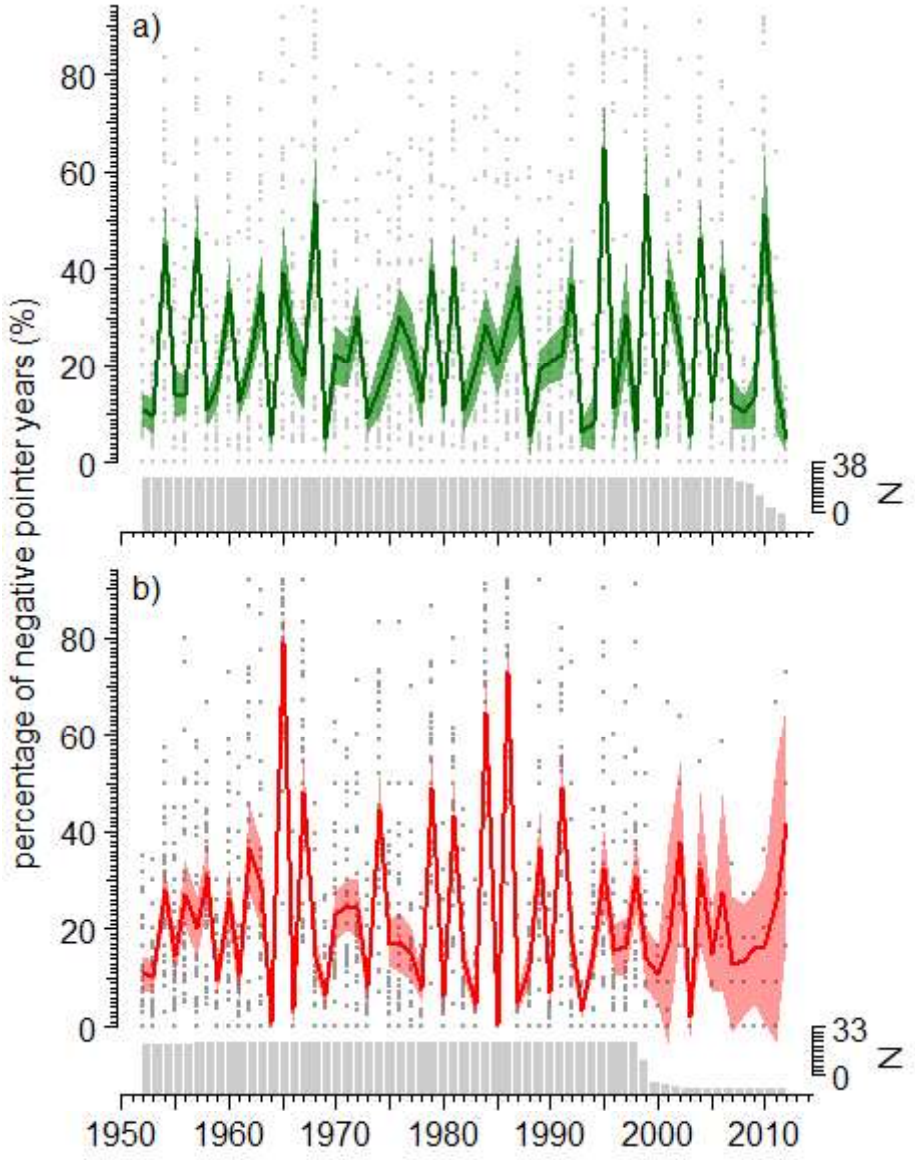

360

361 **Figure 2**. Mean percentage of trees displaying negative pointer years in the two tree
362 species (a, beech; b, Silver fir). Shaded areas represent standard errors. Points indicate
363 site values. Grey bars (secondary y-axis) represent the number of sites (N) with
364 observations for each particular year.

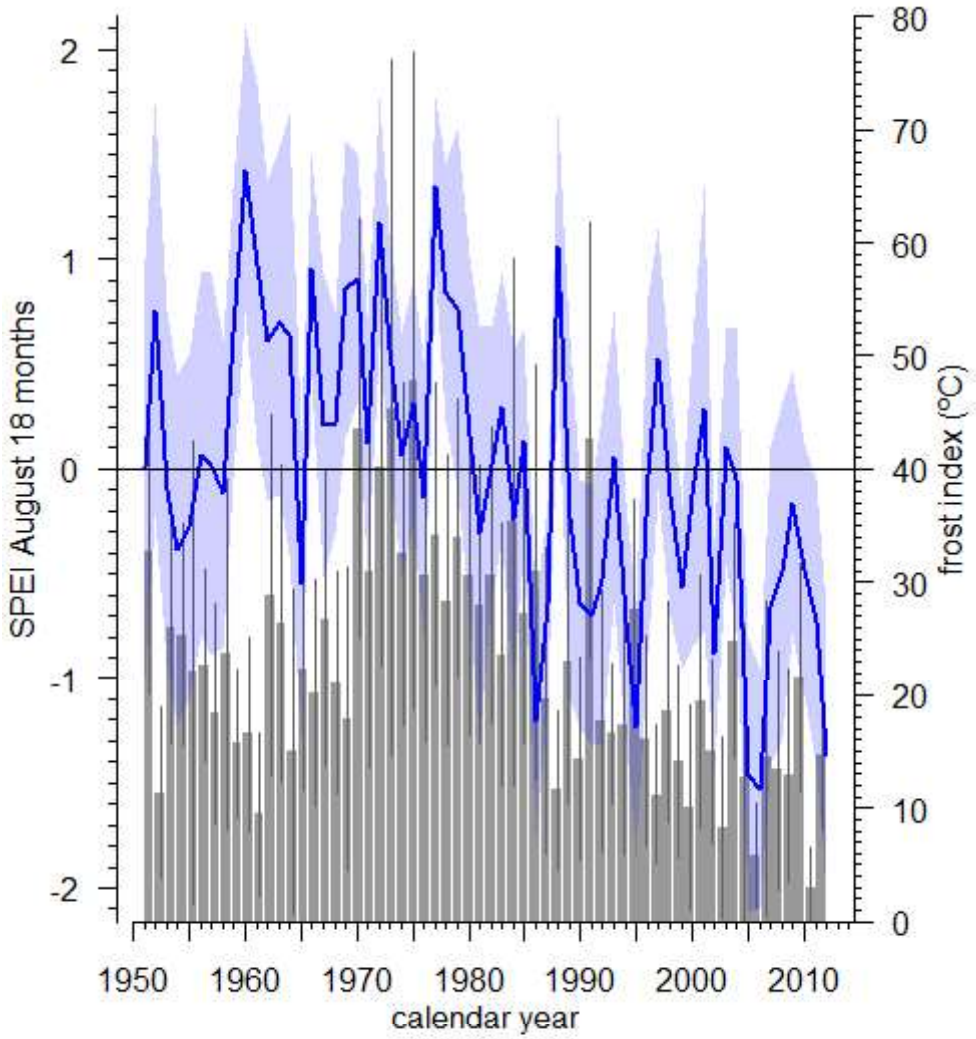

Figure 3. Variability of the 18-month long August SPEI drought index (blue line is the mean) and the frost index (grey bars with higher values indicating higher frost incidence) during the study period (1950-2012). The shaded blue areas represent the standard error for the SPEI mean, and the vertical lines the standard deviation for the frost index.

We found nine Silver fir forests (27%) showing a significant negative correlation between the percentage of trees displaying negative pointer years and the SPEI. Similarly, twelve beech stands (32%) plus twelve silver fir stands (36%) showed a significant positive relationship between the frequency of negative pointer years and

frost index (**Table 2**, **Figure 4**). The correlation between negative pointer years occurrence and 18 month-long August SPEI decreased with longitude and increased with elevation (**Table 3**). Conversely, the correlation between negative pointer years occurrence and frost index increased with latitude and showed a quadratic relationship with site mean average temperature (**Table 3**).

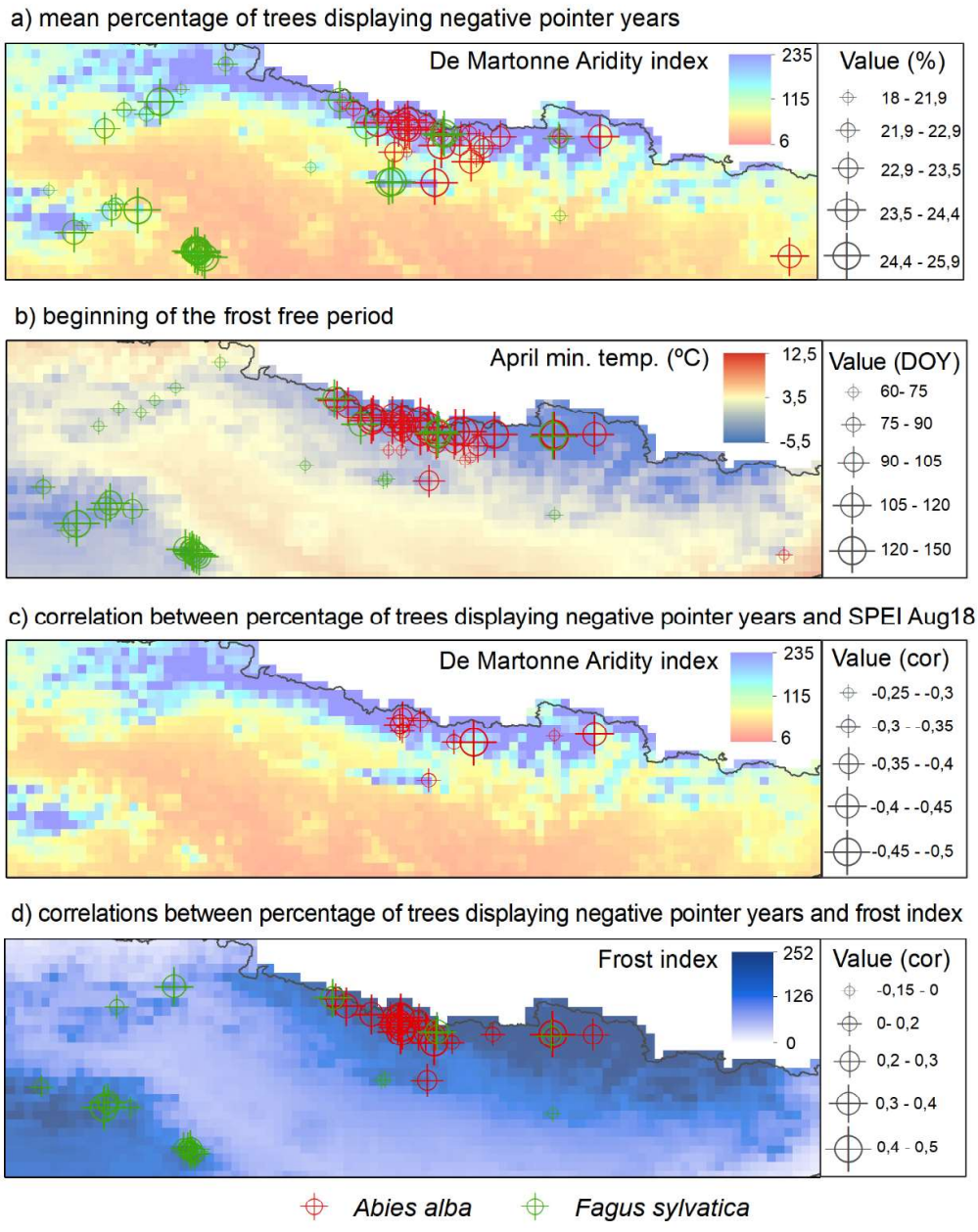

Figure 4. Spatial variation of selected climate variables across the study area in north-eastern Spain: (a), De Martonne aridity index (De Martonne, 1926); (b), April minimum temperatures; (c), De Martonne aridity index; and (d), frost index. The symbols size is

385 proportional to: a) mean percentage of trees displaying negative pointer years; b)
386 beginning of the frost free period in Julian days (DOY); c) correlations between the
387 percentage of trees displaying negative pointer years and 18 month-long August SPEI;
388 and d) correlations between the percentage of trees displaying negative pointer years
389 and the frost index. Red and green symbols indicate the sampled Silver fir and beech
390 forests, respectively.
391

392 **Table 2.** Spearman correlation coefficients (r_s) calculated by relating the occurrence of
393 negative pointer years in radial growth and the 18-month long August SPEI and frost-
394 index.

Tree species	Site	r_s August SPEI	p	r_s frost-index	p
Silver fir	ABAA	-0.2	0.174	0.355	0.013
	ASAA	-0.135	0.359	0.369	0.01
	CAAA	-0.306	0.034	0.432	0.002
	CHAA	-0.229	0.089	0.426	0.001
	COA	-0.162	0.277	0.43	0.003
	MAA	-0.404	0.005	0.271	0.065
	GAAA	-0.149	0.251	0.264	0.04
	GUAA	-0.311	0.034	0.269	0.067
	IAAA	-0.363	0.011	0.414	0.003
	LIAA	-0.36	0.013	0.331	0.023
	LOAA	-0.282	0.055	0.321	0.028
	ORAA	-0.302	0.037	0.179	0.223
	PAAA	-0.332	0.021	0.228	0.119
	SNAA	-0.436	0.002	-0.06	0.684
	SOAA	-0.212	0.152	0.302	0.039
	VIAA	-0.279	0.048	0.405	0.003
	YEAA	-0.243	0.092	0.4	0.004
Beech	COFS	-0.044	0.734	0.275	0.032
	AIFS	-0.067	0.608	0.501	0.000
	DIFS	-0.1	0.446	0.468	0.000
	EAFS	-0.126	0.332	0.33	0.009
	GAFS	-0.048	0.716	0.351	0.006
	L1FS	0.042	0.749	0.366	0.004
	L2FFs	0.004	0.975	0.299	0.021
	M4FS	-0.063	0.636	0.278	0.034
	M5FS	-0.112	0.403	0.278	0.034
	M10F	-0.008	0.953	0.367	0.004
	M17F	-0.083	0.534	0.285	0.030
	OR3F	0.013	0.924	0.319	0.014

395

396 **Table 3.** Results of the linear models selected to study the spatial patterns in the
397 correlations between negative pointer years, drought intensity (18 month-long August
398 SPEI) and frost index. For each variable, the covariates included in the model are

displayed (*t* statistic). The Akaike weight of the model (w_i) and the pseudo-R^2 are displayed. TMed is the mean temperature.

	Elevation	longitude	Latitude	T Med	$TMed^2$	w_i	Pseudo-R^2
r_s SPEI	3.34**	-6.38**	–	–	–	18%	0.38
r_s frost-index	–	–	2.13*	3.82**	-4.37**	15%	0.33

The selected linear mixed-effect model indicated the existence of a positive relationship between the occurrence of negative pointer years and the 18 month-long August SPEI for both species (**Table 4**), confirming that growth was reduced by dry conditions during and before the growing season (**Figure 5**). The strength of the association between drought (SPEI) and the occurrence of negative pointer years was higher in the case of silver fir than in the case of beech (**Table 4; Figure 5**). Similarly, the two tree species showed a positive relationship between the occurrence of negative pointer years and the frost index, indicating that spring late frosts reduced radial growth. However, this effect was slightly stronger in the case of beech than in Silver fir (**Table 4, Figure 5**). The selected model in the case of silver fir accounted for 5% of the variation in the occurrence of negative pointer years (**Table 4**). Similarly, in the case of beech the model accounted for 9% of the variation. The effect of late frosts on growth was twice as important as the drought effect in beech. The interaction between the frost index and the August SPEI was not significant in the selected model.

Table 4. Statistics of the selected linear-mixed effects model fitted to the occurrence of negative pointer years as a function of the 18 month-long August SPEI, the frost index and their interaction. The ΔAICc, Akaike weight (w_i) and pseudo-R^2 of the selected

models are shown. The two values in the last column indicate the marginal and conditional (between parentheses) R^2 values, respectively.

Tree species	Variable	*t* value	*p*	ΔAICc	*wi*	R^2
Silver fir	SPEI	-6.73	< 0.01	1.11	0.64	0.04 (0.05)
	Frost index	5.74	< 0.01			
	Interaction	–	–			
Beech	SPEI	-3.89	< 0.01	0.22	0.53	0.04 (0.09)
	Frost index	7.39	< 0.01			
	Interaction	–	–			

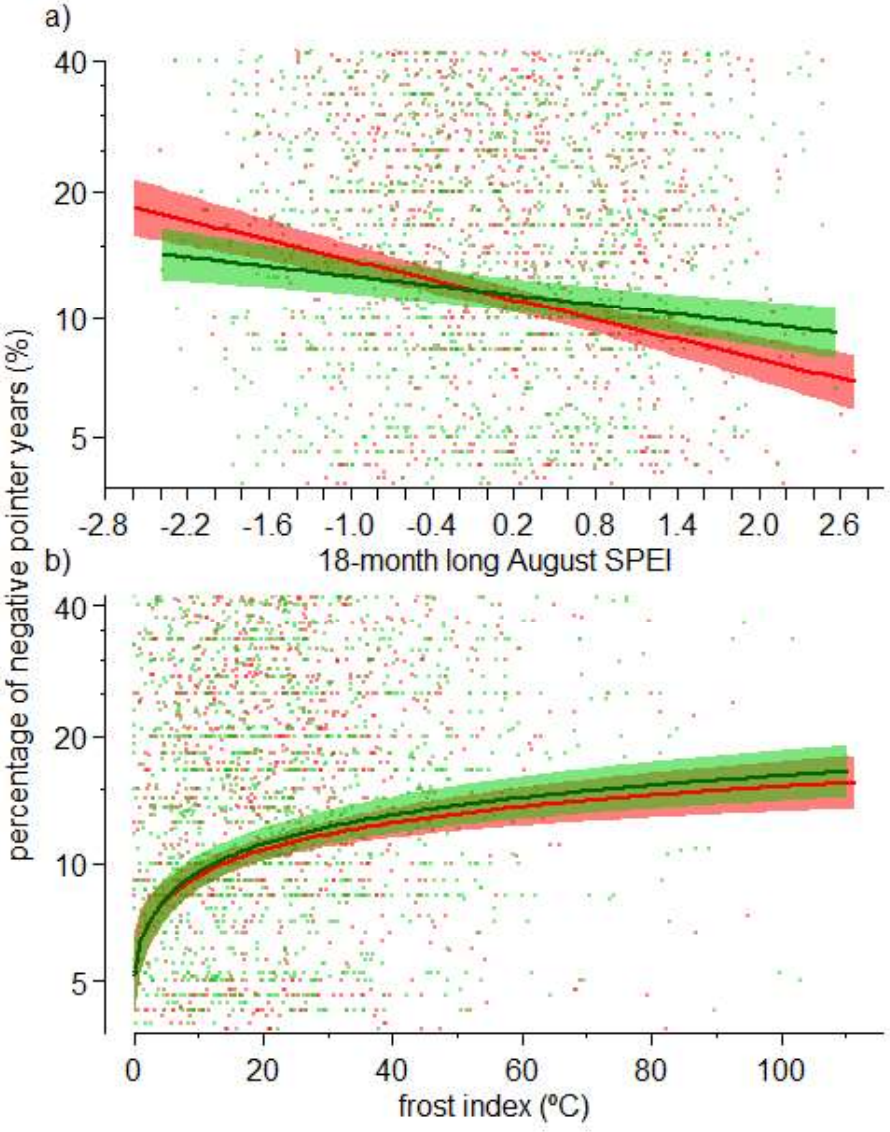

Figure 5. Effects of drought (18-month long August SPEI) and frost index (ºC) on the percentage of negative pointer years in Silver fir (red lines and symbols) and beech

426 (green lines and symbols) according to the selected Linear Mixed-Effect models (see
427 **Table 4**).
428
429 **Discussion**
430 Our results support the hypothesis that the radial growth of Silver fir and beech is
431 negatively impacted by the occurrence of both, late frost events and summer drought
432 near their southernmost distribution limits. The occurrence of negative pointer years in
433 the two species increases with the increase in frost index and decreases with the
434 decrease in 18 month-long August SPEI. We found that the radial growth of beech was
435 particularly susceptible to late frost, thus partially supporting our second hypothesis.
436 However, the lack of a significant interaction between frost index and SPEI do not
437 support the hypothesis that the simultaneous occurrence of these two climate extremes
438 more strongly impacted on growth than their separate incidence. These results shall be
439 interpreted with caution as they can be contingent on the definition of the frost index.
440 Here, we defined the frost-free period as the period without late frost events based on
441 daily climate conditions solely, and thus we lacked information on when leaf unfolding
442 occurs in the sampled sites and during the study period. Further studies considering a
443 more mechanistic definition of the frost-free period and the beginning of the leaf
444 unfolding season using *in situ* phenological records or satellite-derived phenological
445 surrogates may test if the frost index is a valid approach to quantify the occurrence of
446 late frost events and their impact on growth.
447 We found a significant increase in the occurrence of negative pointer years with
448 the decrease in the 18 month-long August SPEI indicating the sensitivity of the radial
449 growth of Silver fir to summer drought in agreement with previous studies (Camarero et
450 al. 2015a, 2015b; Gazol et al., 2015; Gazol et al., 2018; Serra-Maluqer et al., 2019). The

responsiveness of Silver fir to drought could explain the occurrence of dieback episodes on Pyrenean forests which has been observed from the 1980s onwards (Gazol et al., 2015). The post-1970s warming trends and the occurrence of severe droughts have been identified as important factors contributing to this decline (Sangüesa-Barreda et al., 2015). In particular, the severe 1985-1986 drought (see **Figs. 3 and 4**) has been identified as the starting point for this declining trend (Camarero et al., 2011), which was intensified by successive droughts such as those occurring in 2005 and 2012 (Camarero et al., 2015b). Nevertheless, the 1986 spring was very cold in some sites where spring frosts occurred (**Fig. 3**), so the potential interaction between drought and cold stress should be further investigated in those sites. Regarding beech, several studies have also demonstrated that its growth is impaired by summer drought (Rozas, 2003; Rozas et al., 2015; Serra-Maluqer et al., 2019). A recent study considering several populations across north-eastern Spain, suggests that the radial growth of beech is decreasing as a consequence of global warming (Serra-Maluqer et al., 2019). We found that drought intensity has increased in the study region during the last decades (**Table 2**), and that this has reduced the radial growth in beech as confirmed by the linear mixed-effect models. However, the site to site analyses showed no significant influence of SPEI on the occurrence of severe growth reductions in beech. Thus, our results suggest that the radial growth of Silver fir is more sensitive to summer drought than the growth of beech near their southern distribution limits. This situation can be related to the fact that some studied Silver fir forests are situated in regions with dieback episodes occurring during the last decades (e.g. Camarero et al., 2011; Gazol et al., 2015), whilst few beech stands showed symptoms associated to drought-induced dieback (Camarero et al., 2018).

We found that the occurrence of negative pointer years in Silver fir and beech was positively related to the frost index. A similar number of forests of the two species (**Table 2**) showed an impact of the frost index on the occurrence of negative pointer years. However, the fitted models suggest that beech growth is slightly more impacted by late frosts than Silver fir growth (**Table 3**; **Figure 4**). Latreille *et al*. (2017) found a marked sensitivity of Silver fir growth to the occurrence of summer drought and frost along two altitudinal gradients in south-eastern France. Cailleret and Hendrik (2010) found a higher sensitivity of beech to both, summer drought and late frost, along a wide altitudinal and climatic gradient in southern France. In our study, most of the studied Silver fir stands are mountain forests found at intermediate to high elevations (from 918 to 2008 m), whereas beech forests display a greater altitudinal gradient (from 405 to 1850 m) encompassing mountain and lowland forests. This is probably the reason for the strong linkage between the start of the frost-free period and site elevation in the case of beech, whereas in Silver fir it was mainly related with site latitude. These differences together with the widespread decline of silver fir in the region as a consequence of drought could explain the higher sensitivity to drought of Silver fir, and the marked growth responsiveness to frost in beech.

The occurrence of late frost events can impact tree growth negatively due to two mechanisms: frost damage in the bursting buds and expanding leaves and frost-induced xylem embolism (Fernández-Pérez et al., 2018). However, the freezing-tolerance of the study species in winter is much higher that the negative temperatures reached during spring frosts (Sakai and Larcher, 1987). In this sense, it is unlikely that frost-induced xylem embolism (e.g. Camarero et al., 2015a) can be impairing growth in the selected sites. Most likely, negative impacts of frost on drought may occur as a consequence of the death of young leaves just after flushing (Augspurger, 2009). This will explain why

500 the deciduous beech is more sensitive to late frost events than the evergreen Silver fir.
501 However, further research is required to disentangle the mechanisms by which late frost
502 events can reduce growth of these species. Moreover, it is also plausible to think that
503 not all late frost events translate into growth reductions (Puchałka et al., 2016; 2017) as
504 favourable growing seasons can mitigate its impacts. Thus, post-frost resilience
505 mechanisms should also have to be considered including a higher photosynthesis rate
506 and lifespan of second-cohort leaves or an enhanced autumn bud growth, changes which
507 allow compensating for spring frost damage in beech saplings (Zohner et al., 2019). In
508 addition, beech shows a conservative phenology as compared with other tree species
509 (e.g. *Acer* spp.), which leaf out earlier and are more affected by spring frosts (Hufkens
510 et al., 2012; Ma et al., 2019).
511 Evaluating long-term late frost damage on tree performance is challenging as it
512 requires reconstructing phenology and local climate conditions (Augspurger, 2013).
513 This is particularly important mostly considering that different phenological forms of
514 the same species can coexist even within a region (Rubtstov and Utkina, 2008; Kraj and
515 Sztorc, 2009; Utkina and Rubtsov, 2017), and that trees can have local adaptations to
516 tolerate late frost events or to recover after them (Puchałka et al., 2017). In this study,
517 we followed a conservative definition of late frost events by considering that the start of
518 the frost-free period in each site was fixed during the study period (1950-2012), and by
519 considering only the frosts that occurred during this period. The frost-free period started
520 right after early March in only six beech forests with mean annual temperatures above
521 10ºC. Conversely, in eleven Silver fir sites and four beech sites the frost-free period
522 started after early May, and those sites had mean annual temperatures below 6ºC.
523 Probably because of global warming, the occurrence of late frost events, as defined in
524 this study, has decrease in the study region (**Table 2**). However, it is also plausible to

525 think that the phenology of the tree species is changing (Gordo and Sanz, 2010; Vitasse
526 et al., 2014b). Thus, our conservative definition of frost-index could be reformulated
527 considering other factors as the photoperiod (Körner et al., 2016). In addition, better
528 assessments of frost impacts based on remote-sensing or digital camera data may help to
529 advance in this topic (Richardson et al., 2018).

530 To conclude, beech and Silver fir growth was reduced by both late frosts and
531 summer droughts, but not by their interaction. Beech growth was mainly impacted by
532 late frosts, whereas Silver fir growth was more constrained by dry summers despite it
533 also responded to late frost. Further studies should use phenological information to
534 pinpoint frost effects on growth and, and also investigate resilience patterns related to
535 post-frost refoliation.

536

537 **Acknowledgements**

538 We thank all people who helped us in the field and the laboratory, particularly Gabriel
539 Sangüesa-Barreda, Pere Casals and Rubén Camarero Jiménez.

Bibliography

Anderegg, W.R.L., Kane, J.M., Anderegg, L.D.L., 2012. Consequences of widespread tree mortality triggered by drought and temperature stress. Nat. Clim. Ch. 3, 30–36.

Augspurger, C.K., 2009. Spring 2007 warmth and frost: Phenology, damage and refoliation in a temperate deciduous forest. Funct. Ecol. 23, 1031–1039.

Augspurger, C.K., 2013. Reconstructing patterns of temperature, phenology, and frost damage over 124 years: Spring damage risk is increasing. Ecology 94, 41–50.

Barton, K., 2012. MuMIn: Multi-model inference. (R package version 1.7.7) 2012 Available at http://CRAN.R-project.org/package=MuMIn

Bascietto, M., Bajocco, S. Mazzenga, F., Matteucci, G., 2018. Assessing spring frost effects on beech forests in Central Apennines from remotely-sensed data. Agric. For. Meteorol. 248, 240–250.

Bigler, C., Bugmann, H., 2018. Climate-induced shifts in leaf unfolding and frost risk of European trees and shrubs. Sci. Rep. 8, 9865.

Bretz, F., Hothorn, T., Westfall, P., 2010. Multiple Comparisons Using R. Chapman & Hall/CRC Press, Boca Raton, USA.

Bunn, A., Korpela, M., Biondi, F., Campelo, F., Mérian, P., Qeadan, F., et al. 2016. dplR: Dendrochronology Program Library in R. R package version 1.6.4. https://CRAN.R-project.org/package=dplR

Burnham, K.P., Anderson, D.R., 2002. Model Selection and Multimodel Inference: a Practical Information-theoretic Approach. Springer, New York.

Cailleret M., Hendrik, D., 2011. Effects of climate on diameter growth of co-occurring *Fagus sylvatica* and *Abies alba* along an altitudinal gradient. Trees-Struct. Funct. 25, 265–276.

565 Camarero, J.J., Gazol, A., Sancho-Benages S, Sangüesa-Barreda, G., 2015a Know your
566 limits? Climate extremes impact the range of Scots pine in unexpected places.
567 Ann. Bot. 116, 917–927.
568 Camarero, J.J., Gazol, A., Sangüesa-Barreda, G., Oliva, J., Vicente-Serrano, S.M.,
569 2015b. To die or not to die: early-warning signals of dieback in response to a
570 severe drought. J. Ecol. 103, 44–57.
571 Camarero, J.J., Gazol, A., Sangüesa-Barreda, G., Cantero, A., Sánchez-Salguero, R.,
572 Sánchez-Miranda, A., et al., 2018. Forest growth responses to drought at short-
573 and long-term scales in Spain: squeezing the stress memory from tree rings. Front.
574 Ecol. Evol. 6, 9. doi: 10.3389/fevo.2018.00009
575 Camarero, J.J., Gutiérrez, E., 2017. Wood density of silver fir reflects drought and cold
576 stress across climatic and biogeographic gradients. Dendrochronologia 45, 101–
577 112.
578 Caudullo, G., Welk, E., San-Miguel-Ayanz, J., 2017. Chorological maps for the main
579 European woody species. Data in Brief 12, 662–666.
580 Chen, L., Huang, J-G., Ma, Q., Hänninen, H., Rossi, S., Piao, S., Bergeron, Y., 2018.
581 Spring phenology at different altitudes is becoming more uniform under global
582 warming in Europe. Global Ch. Biol. 24, 3969–3975.
583 Cropper, J.P., 1979. Tree-ring skeleton plotting by computer. Tree-Ring Bull. 39, 47–
584 59.
585 Čufar, K., de Luis, M., Prislan, P., Gričar, J., Črepinšek, Z., Merela, M., Kajfež-Bogataj,
586 L., 2015. Do variations in leaf phenology affect radial growth variations in *Fagus*
587 *sylvatica*? Int. J. Biometeorol. 59, 1127–21132.

588 Cuny, H.E., Rathgeber, C.B.K., Lebourgeois, F., Fortin, M., Fournier, M., 2012. Life
589 strategies in intra-annual dynamics of wood formation: example of three conifer
590 species in a temperate forest in north-east France. Tree Physiol. 32, 612–625.
591 De Martonne, E., 1926. Une nouvelle fonction climatologique: L'indice d'aridité. La
592 Meteorol. 449–458.
593 Dittmar, C., Fricke, W., Elling, W., 2006. Impact of late frost events on radial growth of
594 common beech (*Fagus sylvatica* L.) in Southern Germany. Eur. J. For. Res. 125,
595 249–259.
596 Fernández-Pérez, L., Villar-Salvador, P., Martínez-Vilalta, J., Toca, A., Zavala, M.A.,
597 2018. Distribution of pines in the Iberian Peninsula agrees with species
598 differences in foliage frost tolerance, not with vulnerability to freezing-induced
599 xylem embolism. Tree Physiol. 38, 507–516.
600 Frank, D., Reichstein, M., Bahn, M. , Thonicke, K., Mahecha, M. D. et al., 2015.
601 Effects of climate extremes on the terrestrial carbon cycle: concepts, processes
602 and potential future impacts. Glob. Ch. Biol. 21, 2861–2880.
603 Fritts, H.C., 1976. Tree Rings and Climate. Academic Press, London.
604 Fu, Y.H., Zhao, H., Piao, S., Peaucelle, M., Peng, S., Zhou, G., Ciais, P., Huang, M.,
605 Janssens, I. et al., 2015. Declining global warming effects on the phenology of
606 spring leaf unfolding. Nature 526, 104–107.
607 Gazol, A., Camarero, J.J., Gutiérrez, E., Popa, I., Andreu-Hayles, L., Motta, R., et al.,
608 2015. Distinct effects of climate warming on populations of silver fir (*Abies alba*)
609 across Europe. J. Biogeogr. 42, 1150–1162.
610 Gazol, A., Camarero, J.J., Vicente-Serrano, S.M., Sánchez-Salguero, R., Gutiérrez, E.,
611 De Luis, M., et al., 2018. Forest resilience to drought varies across biomes. Glob.
612 Ch. Biol. 24, 2143–2158.

613 Gordo, O., Sanz, J.J., 2010. Impact of climate change on plant phenology in
614 Mediterranean ecosystems. Glob. Ch. Biol. 16, 1082–1106
615 Hänninen, H., 1991. Does climatic warming increase the risk of frost damage in
616 northern trees? Plant, Cell and Env. 14, 449–454. https://doi.org/10.1111/j.1365-
617 3040.1991.tb01514.x
618 Hofmann, M., Bruelheide, H., 2015. Frost hardiness of tree species is independent of
619 phenology and macroclimatic niche. J. Biosci. 40, 147–157.
620 Hofmann, M., Durka, W., Liesebach, M., Bruelheide, H., 2015. Intraspecific variability
621 in frost hardiness of *Fagus sylvatica*. Eur. J. For. Res. 134, 433–441.
622 Hufkens, K., Friedl, M.A., Keenan, T.F., Sonnentag, O., Bailey, A., O'Keefe, J.,
623 Richardson, A.D., 2012. Ecological impacts of a widespread frost event following
624 early spring leaf-out. Glob. Ch. Biol. 18, 2365–2377.
625 IPCC, 2013. Summary for policymakers. In: Climate Change 2013: The Physical
626 Science Basis. Contribution of Working Group I to the Fifth Assessment Report
627 of the Intergovernmental Panel on Climate Change (eds Stocker TF, Qin D,
628 Plattner G-K, Tignor M, Allen SK, Boschung J, Nauels A, Xia Y, Bex V, Midgley
629 PM), pp. 3–29. Cambridge University Press, Cambridge, UK.
630 Keenan, T.F., Gray, J., Friedl, M.A. et al., 2014. Net carbon uptake has increased
631 through warming-induced changes in temperate forest phenology. Nat. Clim. Ch.
632 4, 598–604.
633 Körner, C., Basler, D., Hoch, G., Kollas, C., Lenz, A., Randin, C., Vitasse, Y.,
634 Zimmermann, N.E., 2016. Where, why and how? Explaining the low temperature
635 range limits of temperate tree species. J. Ecol. 104, 1076–1088.
636 Kraj, W., Sztorc, A., 2009. Genetic structure and variability of phenological forms in
637 the European beech (*Fagus sylvatica* L.). Ann. For. Sci. 66, 203.

638 Latreille, A., Davi, H., Huard, F., Pichot, C., 2017. Variability of the climate-radial
639 growth relationship among *Abies alba* trees and populations along altitudinal
640 gradients. For. Ecol. Manage. 396, 150–159.
641 Lenz, A., Hoch, G., Vitasse, Y., Korner, C., 2013. European deciduous trees exhibit
642 similar safety margins against damage by spring freeze events along elevational
643 gradients. New Phytol. 200, 1166–1175.
644 Lenz, A., Hoch, G., Körner, C., Vitasse, Y., 2016. Convergence of leaf-out timing
645 towards minimum risk of freezing damage in temperate trees. Funct. Ecol. 30,
646 1480–1490.
647 Ma, Q., Huang, J.-G., Hänninen, H., Berninger, F.. 2019. Divergent trends in the risk of
648 spring frost damage to trees in Europe with recent warming. Glob. Ch. Biol. 25,
649 351–360.
650 Martinez del Castillo, E., Longares, L.A., Gričar, J., Prislan, P., Gil-Pelegrín, E., Čufar,
651 K., De Luis, M., 2016. Living on the edge: contrasted wood-formation dynamics
652 in *Fagus sylvatica* and *Pinus sylvestris* under Mediterranean conditions. Front.
653 Plant. Sci. 7, 370.
654 Martínez del Castillo, E., Longares, L.A., Serrano-Notivoli, R., Sass-Klaassen, U.G.W.,
655 De Luis, M., 2019a. Spatial patterns of climate-growth relationships across
656 species distribution as a forest management tool in Moncayo Natural Park (Spain).
657 Eur. J. For. Res. https://doi.org/10.1007/s10342-019-01169-3
658 Martínez del Castillo, E., Longares, L.A., Serrano-Notivoli, R., De Luis, M., 2019b.
659 Modeling tree-growth: Assessing climate suitability of temperate forests growing
660 in Moncayo Natural Park (Spain). For. Ecol. Manage. 435, 128–137

Menzel, A., Sparks, T.H., Estrella, N., Koch, E., Aasa, A., Ahas, R. et al.. 2006. European phenological response to climate change matches the warming pattern. Glob. Ch. Biol. 12, 1969–1976.

Nagelkerke, N.J.D., 1991. A note on a general definition of the coefficient of determination. Biometrika 78, 691–692.

Nakagawa, S., Schielzeth, H., 2013. A general and simple method for obtaining R^2 from generalized linear mixed-effects models. Meth. Ecol. Evol. 4, 133–142.

Puchałka, R., Koprowski, M., Przybylak, J., Przybylak, R., Dąbrowski, H.P., 2016. Did the late spring frost in 2007 and 2011 affect tree-ring width and earlywood vessel size in Pedunculate oak (*Quercus robur*) in northern Poland? Int. J. Biometeorol. 60, 1143–1150

Puchałka, R., Koprowski, M., Gričar, J., Przybylak, R., 2017. Does tree-ring formation follow leaf phenology in Pedunculate oak (*Quercus robur* L.)? Eur. J. For. Res. 136, 259–268.

San-Miguel-Ayanz, J., De Rigo, D., Caudullo, G., Houston Durrant, T., Mauri, A. (eds.), 2016. European Atlas of Forest Tree Species. Publication Office of the European Union, Luxembourg.

Serrano-Notivoli, R., Beguería, S., Saz Sánchez, M.A. et al., 2017a. SPREAD: a high-resolution daily gridded precipitation dataset for Spain—an extreme events frequency and intensity overview. Earth Syst. Sci. Data 9, 721–738.

Serrano-Notivoli, R., De Luis, M., Beguería, S.. 2017b. An R package for daily precipitation climate series reconstruction. Env. Model Softw. 89, 190–195.

Serrano-Notivoli, R., Beguería, S., De Luis, M., 2019. STEAD: A high-resolution daily gridded temperature dataset for Spain. Earth Syst. Sci. Data essd-2019-52.

685 Pinheiro, J.C., Bates D.M., 2000. Mixed-Effects Models in S and S-PLUS. Springer-
686 Verlag, New York.
687 Pinheiro, J., Bates, D., DebRoy, S., Sarkar, D., 2014. nlme: Linear and Nonlinear Mixed
688 Effects Models. R package version 3.1-117.
689 Príncipe, A., van der Maaten, E., van der Maaten-Theunissen, M., Struwe, T.,
690 Wilmking, M., Kreyling, J., 2017. Low resistance but high resilience in growth of
691 a major deciduous forest tree (*Fagus sylvatica* L.) in response to late spring frost
692 in southern Germany. Trees-Struct Funct 31, 743–751.
693 R Core Team., 2017. R: A language and environment for statistical computing. R
694 Foundation for Statistical Computing, Vienna, Austria.
695 Richardson, A.D., Hufkens, K., Milliman, T., Aubrecht, D.M., Chen, M., Gray, J.M.,
696 Johnston, M. R., Keenan, T.F., Klosterman, S.T., Kosmala, M., Melaas, E.K.,
697 Friedl, M. A., Frolking, S., 2018. Tracking vegetation phenology across diverse
698 North American biomes using PhenoCam imagery. Sci. Data 5: 180028. Doi
699 10.1038/sdata.2018.28.
700 Robson T.M., Rasztovits E., Aphalo P.J., Alia R., Aranda I., 2013. Flushing phenology
701 and fitness of European beech (*Fagus sylvatica* L.) provenances from a trial in La
702 Rioja, Spain, segregate according to their climate of origin. Agric. For. Meteorol.
703 180, 76–85.
704 Rozas, V., 2003. Regeneration patterns, dendroecology, and forest-use history in an old-
705 growth beech-oak lowland forest in Northern Spain. For. Ecol. Manage. 182, 175–
706 194.
707 Rozas, V., Camarero, J.J., Sangüesa-Barreda, G., Souto, M., García-González, I., 2015.
708 Summer drought and ENSO-related cloudiness distinctly drive *Fagus sylvatica*

709 growth near the species rear-edge in northern Spain. Agric. For. Meteorol. 201,
710 153–164.
711 Rubtsov, V.V., Utkina, I.A. 2008. Adaptatsionnye reaktsii duba na defoliatsiyu
712 (Adaptive Reaction of Oak on Defoliation), Moscow.
713 Sakai, A., Larcher, W. 1987. Frost Survival of Plants, Responses and Adaptation to
714 Freezing Stress. Springer, New York.
715 Sánchez-Gómez, D., Robson, T.M., Gasco, A., Gil-Pelegrin, E., Aranda, I., 2013.
716 Differences in the leaf functional traits of six beech (*Fagus sylvatica* L.)
717 populations are reflected in their response to water limitation. Env. Exp. Bot. 87,
718 110–119.
719 Schweingruber, F.H., Eckstein, D., Serre-Bachet, F., Bräker, O.U., 1990. Identification,
720 presentation and interpretation of event years and pointer years in
721 dendrochronology. Dendrochronologia 8, 9–38.
722 Serra-Maluquer, X., Gazol, A., Sangüesa-Barreda, G., Sánchez-Salguero, R., Rozas, V.,
723 Colangelo, M., Gutiérrez, E., Camarero, J.J., 2019. Geographically structured
724 growth decline of rear-edge Iberian *Fagus sylvatica* forests after the 1980s shift
725 toward a warmer climate. Ecosystems https://doi.org/10.1007/s10021-019-00339-
726 z
727 Spulak, O., Martincova, J., 2015. The influence of the method of silver fir growing and
728 nutrition on sprouting and chlorophyll fluorescence during spring. J. For. Sci. 61,
729 80–88.
730 Suvanto, S., Henttonen, H.M., Nöjd, P., Helama, S., Repo, T., Timonen, M., Mäkinen,
731 H., 2017. Connecting potential frost damage events identified from
732 meteorological records to radial growth variation in Norway spruce and Scots
733 pine. Trees-Struct Funct 31, 2023–2034.

734 Utkina, I., Rubtsov, V., 2017. Studies of phenological forms of pedunculate oak.
735 Contemporary Problems of Ecology 10, 804–811.
736 van der Maaten-Theunissen, M., van der Maaten, E., Bouriaud, O., 2015. pointRes: An
737 R package to analyze pointer years and components of resilience.
738 Dendrochronologia 35, 34–38.
739 Vanoni, M., Bugmann, H., Nötzli, M., Bigler, C., 2016. Drought and frost contribute to
740 abrupt growth decreases before tree mortality in nine temperate tree species. For.
741 Ecol. Manage. 382, 51–63.
742 Vicente-Serrano, Beguería, S., López-Moreno, J.I., 2010. A Multi-scalar drought index
743 sensitive to global warming: The Standardized Precipitation Evapotranspiration
744 Index – SPEI. J. Clim. 23, 1696–1718.
745 Vicente-Serrano, S.M., Gouveia, C., Camarero, J.J., Beguería, S., Trigo, R., López-
746 Moreno, J.I., et al., 2013. Response of vegetation to drought time-scales across
747 global land biomes. Proc. Natl. Acad. Sci. U S A. 110, 52–57.
748 Vitasse, Y., Rebetez, M., 2018. Unprecedented risk of spring frost damage in
749 Switzerland and Germany in 2017. Clim. Ch. 149, 233–246.
750 Vitasse, Y., Schneider, L., Rixen, C., Christen, D., Rebetez, M., 2018. Increase in the
751 risk of exposure of forest and fruit trees to spring frosts at higher elevations in
752 Switzerland over the last four decades. Agric. For. Meteorol. 248, 60–69.
753 Vitasse, Y., Lenz, A., Hoch, G., Körner, C., Piper, F., 2014a. Earlier leaf-out rather than
754 difference in freezing resistance puts juvenile trees at greater risk of damage than
755 adult trees. J Ecol. 102, 981–988.
756 Vitasse, Y., Lenz, A., Körner, C., 2014b. The interaction between freezing tolerance and
757 phenology in temperate deciduous trees. Front. Plant. Sci. 5, 541.

Vitra, A., Lenz, A., Vitasse, Y., 2017. Frost hardening and dehardening potential in temperate trees from winter to budburst. New Phytol. 216, 113–123.

Weigel. R, Muffler, L., Klisz, M., Kreyling, J., van der Maaten-Theunissen, M., Wilmking, M., van der Maaten, E., 2018. Winter matters: Sensitivity to winter climate and cold events increases towards the cold distribution margin of European beech (*Fagus sylvatica* L.). J Biogeogr. 45, 2779–2790. https://doi.org/10.1111/jbi.13444.

Zohner, C.M., Rockinger, A., Renner, S.S., 2019. Increased autumn productivity permits temperate trees to compensate for spring frost damage. New Phytol. 221, 789–795.

Zuur, A.F., Ieno, E.N., Walker, N., Saveliev, A.A., Smith, G.M., 2009. Mixed Effects Models and Extensions in Ecology with R. Springer.Zuur, A.F, Ieno, E.N., Elphick, C.S., 2010. A protocol for data exploration to avoid common statistical problems. Methods Ecol. Evol. 1, 3–14.

773

774 **Supporting Information** of the manuscript "Summer drought and spring frost, but not
775 their interaction, constrain European beech and Silver fir growth in their southern
776 distribution limits" submitted to *Agricultural and Forest Meteorology* by Gazol et al.

777 **Table S1.** Geographic and climatic characteristics of the study sites. Abbreviations: T, mean
778 annual temperature; P, mean annual precipitation; Frost index, day-degrees" below zero from
779 the first day after the frost season to late summer (º C); freefrost, beginning of the frost free
780 period in Julian days; SPEI8, Minimum 18 month-long August Standardized Precipitation
781 Evapotranspiration Index.

Site (province)	Site code	Latitude (N)	Longitude (-W, +E)	Elevation (m)	T (ºC)	P (mm)	Frost index (ºC)	freefrost	SPEI18
Silver fir									
Los Abetazos (Huesca)	ABAA	42.72	-0.32	1403	7.8	1559	14.52	110	-2.35
Paco Asieso (Huesca)	ASAA	42.65	-0.18	1327	6.2	1925	19.03	122	-2.35
Azirón (Huesca)	AZAA	42.65	0.13	1613	5.1	1384	19.91	129	-2.00
Ballibierna (Huesca)	BAAA	42.63	0.35	1600	5.6	1315	17.22	128	-2.59
Bujaruelo (Huesca)	BUAA	42.68	-0.12	1233	6.1	1345	18.65	122	-2.44
Castiello de Jaca (Huesca)	CAAA	42.65	-0.31	1175	8.4	1211	19.07	104	-2.00
El Chate (Huesca)	CHAA	42.57	-0.07	937	8.4	1235	18.79	105	-2.06
Conangles-2 (Lleida)	COAA	42.62	0.78	1635	3.8	2227	27.91	133	-1.91
Diazas (Huesca)	DIAA	42.63	-0.06	1528	5.8	1583	20.19	124	-2.29
Conangles-1 (Lleida)	CNAA	42.63	0.78	1753	3.8	2227	27.91	133	-1.91
Mata de València-High (Lleida)	MAAA	42.63	1.07	2008	7.2	783	18.64	113	-2.32
Montseny (Barcelona)	MTAA	41.77	2.43	1550	9.8	882	28.80	70	-1.86
Collado de Cullibert (Huesca)	VIAA	42.47	0.18	1474	11.3	894	21.33	72	-2.15
Fago (Huesca)	FAAA	42.73	-0.53	918	5.6	1869	24.10	122	-1.91
Gamueta (Huesca)	GAAA	42.88	-0.78	1400	6.6	2606	22.07	112	-1.62
Guara (Huesca)	GUAA	42.3	-0.12	1428	8.6	1658	27.78	91	-2.21
Izquierda de Aragón (Huesca)	IAAA	42.75	-0.31	1478	7.8	1559	14.52	110	-2.35
San Juan de la Peña (Huesca)	JPAA	42.52	-0.41	1393	10.8	741	28.45	71	-2.22
Lierdes (Huesca)	LIAA	42.7	-0.33	1222	8.5	1131	16.96	104	-2.22
Lopetón (Huesca)	LOAA	42.77	-0.52	1009	6.6	1818	21.54	113	-2.18
Monestero (Huesca)	MOAA	42.65	0.07	1400	4.3	1822	26.78	131	-2.16
Peña Oroel (Huesca)	OOAA	42.52	-0.32	1604	10.6	790	29.01	72	-2.20
Orús (Huesca)	ORAA	42.57	0.06	1370	9.2	1140	26.79	92	-2.15
Panticosa (Huesca)	PAAA	42.73	-0.18	1280	3.4	2007	20.87	143	-1.94
Puente Corralones (Huesca)	PCAA	42.77	-0.38	1248	6.4	1574	23.77	113	-1.88
Paco Ezpela (Huesca)	PEAA	42.75	-0.52	1232	5.6	1869	24.10	122	-1.91
Paco Mayor (Huesca)	PMAA	42.7	-0.38	1353	6.3	1662	20.61	118	-1.87
Peña Montañesa (Huesca)	PNAA	42.45	0.14	1519	11.5	868	20.32	71	-2.08

Collado de Sahún (Huesca)	SAAA	42.55	0.23	1789	8.5	1162	18.92	105	-1.69
Selva Negra (Huesca)	SNAA	42.57	0.2	1431	10.9	1075	26.12	72	-2.22
Selva de Oza (Huesca)	SOAA	42.83	-0.7	1272	6.5	2738	22.36	113	-1.57
Paco de Villanúa (Huesca)	VNAA	42.68	-0.3	1270	8.5	1131	16.96	104	-2.22
Yésero (Huesca)	YEAA	42.65	-0.13	1399	7.1	1335	20.29	113	-2.28
European beech									
Sierra Cebollera (Soria)	CEFS	41.99	-2.65	1638	6.7	1771	16.75	122	-2.13
Conangles (Lleida)	COFS	42.62	0.77	1635	3.8	2227	27.91	133	-1.91
Aisa (Huesca)	AIFS	42.7	-0.61	1147	8.1	1675	18.73	107	-2.22
Bértiz (Navarra)	BEFS	43.15	-1.62	405	12.4	2266	6.97	61	-1.87
Diustes (Soria)	DIFS	42.1	-2.44	1400	8.0	962	16.68	107	-2.17
Eraso (Navarra)	EAFS	42.97	-1.94	650	9.7	1535	25.88	61	-1.88
Gamueta (Huesca)	GAFS	42.89	-0.8	1400	6.6	2606	22.07	112	-1.62
Izki (Alava)	IZFS	42.69	-2.49	760	10.9	818	18.67	61	-1.71
Lokiz (Navarra)	LOFS	42.79	-2.19	1050	11.0	942	15.25	61	-1.86
Luesia (Zaragoza)	LUFS	42.41	-1.01	1050	10.5	1202	27.52	61	-2.13
Monrepos (Huesca)	MOFS	42.31	-0.42	1560	10.3	1541	26.33	71	-2.24
Montsec (Lleida)	MTFS	42.06	0.78	1360	10.9	598	24.14	68	-1.79
Opakua (Alava)	OPFS	42.82	-2.35	1000	10.8	936	15.90	61	-1.87
Peiró (Huesca)	PEFS	42.3	-0.45	1380	10.3	1541	26.33	71	-2.24
Urbasa (Navarra)	URFS	42.88	-2.09	1000	9.2	1339	26.71	68	-1.65
Hayedo de Santiago-high (La Rioja)	L1FS	42.14	-2.41	1600	7.8	1166	16.09	109	-1.79
Hayedo de Santiago-low (La Rioja)	L2FS	42.14	-2.41	1360	8.1	1025	16.31	107	-1.96
Fuente la Teja-Moncayo (Zaragoza)	M01FS	41.8	-1.82	1200	9.6	831	34.29	76	-2.03
Peña Roya (PN Moncayo)	M02FS	41.81	-1.84	1400	8.8	1058	18.00	103	-1.92
Peña Nariz (PN Moncayo)	M03FS	41.8	-1.82	1600	8.1	1270	19.18	109	-1.92
Barranco de Apio - Moncayo (Zaragoza)	M04FS	41.78	-1.81	1420	8.4	1187	17.79	108	-1.82
Val de Manzano (PN Moncayo)	M05FS	41.77	-1.79	1500	8.2	1229	19.02	109	-1.88
Hoya el Cerezo -Moncayo (Zaragoza)	M06FS	41.77	-1.76	1170	10.1	642	31.47	72	-2.11
Haya Seca -Moncayo (Zaragoza)	M10FS	41.8	-1.82	1600	8.1	1270	19.18	109	-1.92
Fuente la Teja-Moncayo (Zaragoza)	M11FS	41.81	-1.82	1200	9.9	718	34.00	72	-2.24
Collado la Lona-Moncayo (Zaragoza)	M14FS	41.76	-1.77	1440	8.5	1162	17.89	107	-1.91
Arroyo de Castilla-Moncayo (Zaragoza)	M16FS	41.81	-1.84	1150	10.0	680	32.69	72	-2.27
Arroyo los Cejos-Moncayo (Zaragoza)	M17FS	41.81	-1.87	1520	8.5	1165	16.61	107	-1.79
Barranco Castilla-Moncayo (Zaragoza)	M26FS	41.81	-1.84	1380	8.8	1058	17.63	103	-1.88
Barranco de Castilla-Moncayo (Zaragoza)	M27FS	41.81	-1.84	1320	9.2	978	26.49	91	-1.90
Barranco de Castilla-Moncayo (Zaragoza)	M28FS	41.81	-1.83	1255	9.6	841	34.19	76	-2.09
Barranco de Castilla-Moncayo (Zaragoza)	M29FS	41.81	-1.82	1177	9.9	718	34.00	72	-2.24
Senda Cazadores-Ordesa (Huesca)	O01FS	42.64	-0.06	1850	5.8	1583	20.19	124	-2.29
Senda Cazadores-Ordesa (Huesca)	O02FS	42.64	-0.06	1750	5.8	1583	20.19	124	-2.29
Senda Cazadores-Ordesa (Huesca)	O03FS	42.65	-0.05	1400	7.3	1621	19.43	113	-2.05
Poyales (La Rioja)	POFS	42.1	-2.25	1268	8.5	1227	24.47	96	-1.77
Valle del Rio Razón (Soria)	RAFS	41.94	-2.71	1493	9.1	1000	39.08	79	-2.38
El Rajao (La Rioja)	RJFS	42.25	-2.89	1147	8.7	832	42.05	77	-1.91

782

783

784 **Table S2.** Characteristics of the tree-ring width (TRW) series. Abbreviations: SD,
785 standard deviation, Rbar, mean correlation between series; AR1, first-order
786 autocorrelation.
787

Species	Site code	No. radii	Start	End	Mean TRW (mm)	SD TRW (mm)	Rbar	AR1	Negative pointer years (%)
Silver fir	ABAA	24	1889	2000	4.46	2.28	0.55	0.83	20.56
	ASAA	20	1869	2000	3.05	1.82	0.60	0.84	18.01
	AZAA	22	1870	2000	3.29	1.40	0.58	0.78	23.01
	BAAA	29	1861	2000	2.09	0.86	0.62	0.80	22.99
	BUAA	12	1919	2017	2.57	1.57	0.51	0.89	23.23
	CAAA	20	1834	2000	1.23	0.81	0.57	0.80	22.40
	CHAA	11	1956	2017	2.88	1.12	0.65	0.70	25.45
	COAA	12	1850	2017	2.37	1.73	0.43	0.82	21.82
	DIAA	24	1860	2000	2.66	1.31	0.67	0.79	21.57
	CNAA	20	1662	1999	0.83	0.49	0.55	0.88	22.55
	MAAA	35	1767	1999	0.89	0.51	0.63	0.84	23.40
	MTAA	30	1587	1999	1.11	0.85	0.54	0.84	23.64
	VIAA	27	1819	2000	2.75	1.71	0.49	0.81	21.36
	FAAA	24	1883	2000	2.83	1.29	0.72	0.75	25.52
	GAAA	33	1785	2017	1.82	1.20	0.59	0.82	21.66
	GUAA	23	1858	1999	2.92	1.46	0.68	0.65	25.30
	IAAA	25	1777	2000	2.70	1.74	0.59	0.79	23.93
	JPAA	28	1855	1999	2.16	1.50	0.55	0.83	23.31
	LIAA	22	1876	1999	2.96	1.79	0.57	0.84	24.90
	LOAA	23	1875	1999	1.42	1.02	0.64	0.76	21.72
	MOAA	30	1769	1999	1.54	0.90	0.51	0.85	23.04
	OOAA	47	1889	2000	2.70	1.31	0.69	0.75	21.89
	ORAA	22	1872	2000	1.73	0.66	0.64	0.71	23.44
	PAAA	24	1824	2000	2.44	1.48	0.69	0.80	23.18
	PCAA	27	1896	1999	3.49	2.15	0.56	0.78	22.33
	PEAA	71	1842	2002	1.58	0.98	0.58	0.78	21.07
	PMAA	22	1886	1999	1.97	0.97	0.72	0.63	24.23
	PNAA	22	1895	2001	2.64	1.42	0.61	0.74	24.49
	SAAA	29	1667	2000	1.87	1.48	0.56	0.81	22.94
	SNAA	29	1903	2000	2.89	1.37	0.65	0.81	23.43
	SOAA	51	1771	1999	2.15	1.72	0.54	0.86	22.37
	VNAA	42	1874	2003	1.99	1.15	0.58	0.80	24.08
	YEAA	24	1920	2001	3.44	1.68	0.64	0.74	22.81
European beech	CEFS	21	1933	2017	1.68	1.24	0.41	0.68	22.42
	COFS	12	1856	2017	1.60	1.02	0.51	0.68	23.09
	AIFS	27	1915	2016	1.26	0.71	0.55	0.65	24.77
	BEFS	38	1857	2008	1.54	1.38	0.58	0.81	22.85
	DIFS	14	1918	2012	1.71	1.09	0.64	0.81	23.10
	EAFS	40	1887	2016	1.72	1.16	0.36	0.68	21.42
	GAFS	49	1701	2017	1.09	0.93	0.57	0.53	23.94

IZFS	39	1871	2008	2.71	1.63	0.66	0.77	23.08
LOFS	24	1830	2017	1.28	0.86	0.49	0.65	20.38
LUFS	24	1918	2012	1.85	1.12	0.67	0.78	21.32
MOFS	22	1897	2009	1.34	0.91	0.55	0.66	24.30
MTFS	19	1868	2016	1.72	1.07	0.53	0.69	21.35
OPFS	33	1798	2016	1.41	0.83	0.51	0.64	21.56
PEFS	12	1877	2011	2.03	1.23	0.60	0.72	24.04
URFS	40	1816	2008	2.04	1.21	0.61	0.65	24.51
L1FS	22	1661	2012	1.10	0.79	0.60	0.59	22.88
L2FS	22	1878	2011	1.61	0.81	0.72	0.66	22.50
M01FS	35	1902	2014	1.38	0.85	0.62	0.78	22.54
M02FS	19	1829	2010	0.74	0.53	0.67	0.76	23.50
M03FS	14	1832	2011	0.71	0.49	0.65	0.66	24.89
M04FS	20	1835	2010	1.24	0.88	0.66	0.70	23.16
M05FS	30	1912	2010	1.41	0.85	0.60	0.64	23.59
M06FS	10	1914	2010	1.76	1.14	0.66	0.79	19.20
M10FS	40	1799	2014	0.78	0.45	0.64	0.72	25.16
M11FS	20	1904	2010	1.47	0.85	0.61	0.70	23.02
M14FS	10	1939	2010	1.49	0.78	0.57	0.56	25.73
M16FS	19	1902	2010	1.06	0.68	0.59	0.70	23.41
M17FS	20	1887	2010	1.84	0.94	0.62	0.57	23.28
M26FS	12	1825	2011	0.95	0.64	0.59	0.75	22.74
M27FS	11	1830	2011	0.96	0.54	0.58	0.72	24.04
M28FS	12	1836	2011	1.02	0.52	0.61	0.65	22.74
M29FS	12	1904	2011	1.59	0.80	0.67	0.73	24.58
O01FS	15	1903	2011	1.41	0.56	0.50	0.56	23.50
O02FS	20	1719	2011	0.79	0.41	0.62	0.65	23.77
O03FS	22	1883	2011	1.86	0.88	0.50	0.61	23.74
POFS	24	1785	2017	0.90	0.57	0.48	0.63	25.15
RAFS	28	1892	2017	1.31	0.73	0.54	0.78	24.23
RJFS	24	1704	2017	1.56	1.11	0.47	0.77	21.72

788

789

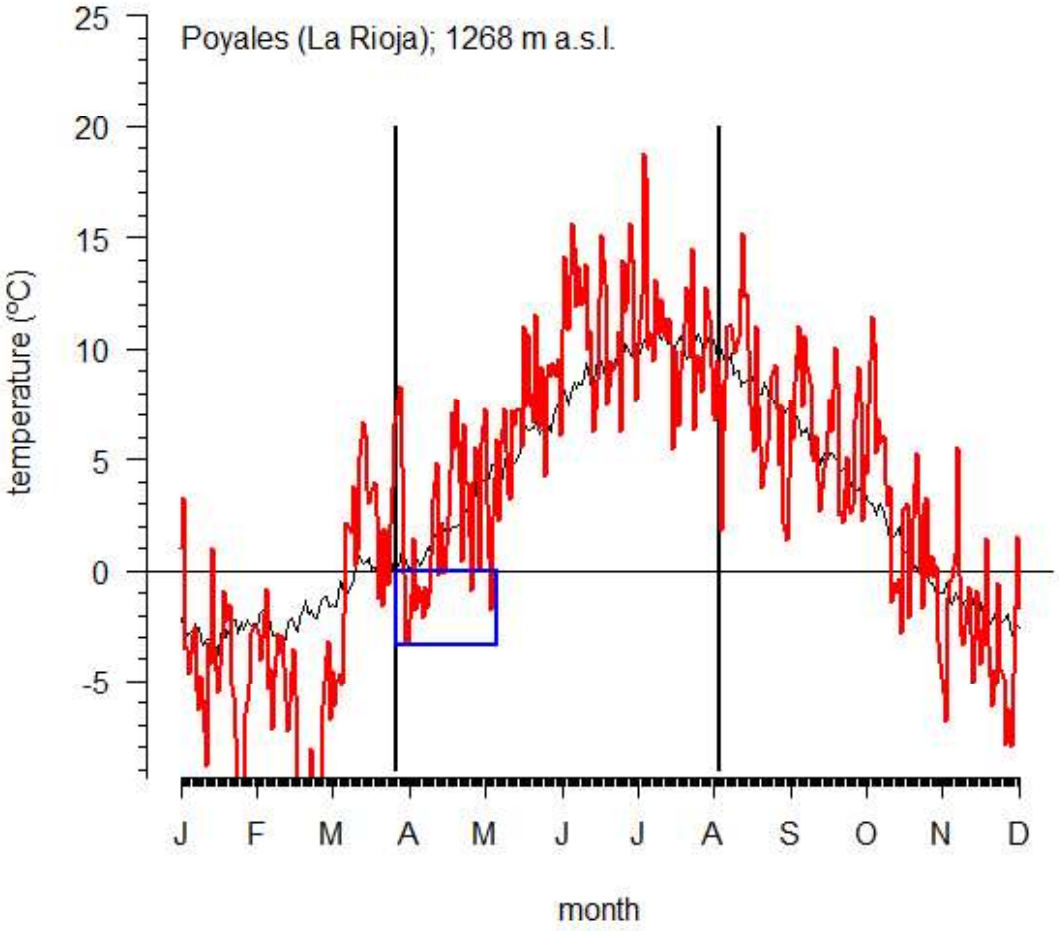

Figure S1. Calculation of the frost index for the 2005 year in the Poyales beech study site. The black line represents the average daily minimum temperature for the period 1950-2012 along the year. The black vertical line in late March represents the beginning of the site-specific frost-free period, whereas the August vertical line represents the end of the studied period. The red line represents the daily minimum temperature for the year 2005. The blue line overlapping the red line during April indicates the occurrence of a late frost event (i.e. days with daily mean temperature below zero in the site specific frost-free period before summer).